

## Structure–activity relationships of novel inhibitors of glyceraldehyde-3-phosphate dehydrogenase

Andrei Leitão,<sup>a</sup> Adriano D. Andricopulo,<sup>b</sup> Glaucius Oliva,<sup>b</sup> Mônica T. Pupo,<sup>c</sup>  
Anderson A. de Marchi,<sup>c</sup> Paulo C. Vieira,<sup>d</sup> Maria Fátima G. F. da Silva,<sup>d</sup>  
Vitor F. Ferreira,<sup>e</sup> Maria Cecília B. V. de Souza,<sup>e</sup> Marcus M. Sá,<sup>f</sup>  
Valéria R. S. Moraes<sup>g</sup> and Carlos A. Montanari<sup>a,\*</sup>

<sup>a</sup>Núcleo de Estudos em Química Medicinal-NEQUIM, Departamento de Química,  
Universidade Federal de Minas Gerais, 31270-901 Belo Horizonte-MG, Brazil

<sup>b</sup>Centro de Biotecnologia Molecular Estrutural-CBME, Instituto de Física de São Carlos,  
Universidade de São Paulo, 13566-590 São Carlo-SP, Brazil

<sup>c</sup>Faculdade de Ciências Farmacêuticas, Universidade de São Paulo, 14040-903 Ribeirão Preto-SP, Brazil

<sup>d</sup>Departamento de Química, Universidade Federal de São Carlos, 13565-905 São Carlos-SP, Brazil

<sup>e</sup>Instituto de Química, Universidade Federal Fluminense, 24020-150 Niterói, RJ, Brazil

<sup>f</sup>Departamento de Química, Universidade Federal de Santa Catarina, 88040-900 Florianópolis-SC, Brazil

<sup>g</sup>Departamento de Química, Universidade Federal de Sergipe, 49100-000 São Cristovão-SE, Brazil

Received 1 November 2003; revised 5 February 2004; accepted 5 February 2004

**Abstract**—3D QSAR studies were performed on a library of 120 GAPDH inhibitors, including a series of coumarins, flavonoids, and nucleosides. The VolSurf method was successfully used to calculate surface descriptors for protein–ligand affinity and binding site of the enzyme. PCA/PLS analyses have permitted the evaluation of the structural features crucial for potency, selectivity, and favorable pharmacokinetic properties, and are important for the design of new ligands.

© 2004 Elsevier Ltd. All rights reserved.

Chagas disease, also known as American trypanosomiasis, is an infection caused by the protozoan parasite *Trypanosoma cruzi*. According to the World Health Organization (WHO), the disease affects 16–18 million people, and about 25% of the population of Central and South America is at risk of contracting the infection.<sup>1</sup> However, despite the public threat posed by the disease, currently available drugs (e.g., benznidazole and nifurtimox, the latter no longer being available) are inadequate and their impact is often limited by serious adverse effects, toxicity, and ineffectiveness. Clearly, there is a critical need for new drugs with different mechanisms of action for the treatment of Chagas disease.<sup>1</sup>

The bloodstream stage of *T. cruzi* is highly dependent on glycolysis for energy production. Accordingly, the

inhibition of enzymes of this physiologically important metabolic pathway should deprive the parasite of the energy necessary for survival. The glycosomal glyceraldehyde-3-phosphate dehydrogenase (gGAPDH) is an attractive target for the development of novel anti-trypanosomatid agents.<sup>2</sup> This enzyme catalyzes the reversible oxidative phosphorylation of glyceraldehyde-3-phosphate to 1,3-bisphosphoglycerate in the presence of NAD<sup>+</sup> and inorganic phosphate.<sup>3</sup>

The crystal structures of GAPDH from several species have been determined, including among others: human,<sup>4</sup> *T. brucei*,<sup>5</sup> *T. cruzi*,<sup>6a,b</sup> and *Leishmania mexicana*.<sup>7</sup> While the overall structures of the parasite enzymes are very similar, they are significantly different from the human counterpart.<sup>8,9</sup>

Recently, we have reported the virtual screening of a large chemical database against *T. cruzi* GAPDH. A number of ligands were selected and further investigated using the VolSurf method.<sup>10</sup> The study yielded

**Keywords:** Chagas disease; Enzyme inhibitors; 3D QSAR.

\*Corresponding author. Tel.: +55-3134995728; fax: +55-3134995700;  
e-mail: [montana@dedalus.lcc.ufmg.br](mailto:montana@dedalus.lcc.ufmg.br)

interesting insights on the 3D molecular field requirements for binding affinities. The successful use of the VolSurf method to calculate surface descriptors for protein–ligand affinity encouraged us to further extend our investigations. In the present work, we describe the use of the VolSurf method to explore the structure–activity relationships of a new series of GAPDH inhibitors, employing H<sub>2</sub>O and hydrophobic DRY probes as earlier described.<sup>10</sup> Moreover, pharmacokinetic properties were also evaluated by using the VolSurf method.<sup>11</sup> The data set consists of 120 structurally diverse inhibitors, including a series of coumarins, flavonoids, and nucleosides. The results of the principal component analysis (PCA) performed on the 67 coumarins contained in the data set are shown in Figure 1.

The figure shows the PC1 versus PC2 score plot with the coumarins clustered in the region of high positive values of PC1 (30% of the variance). These findings corroborate those of earlier studies,<sup>10</sup> where the most potent coumarins are clustered in a similar fashion. The classification is of particular interest since PCA does not explicitly consider the activity of the compounds. However, PCA was able to divide the molecules in such a way that the biological activity was recognized in a correct ranking order around the series of compounds. Based on these results, we have synthesized and evalu-

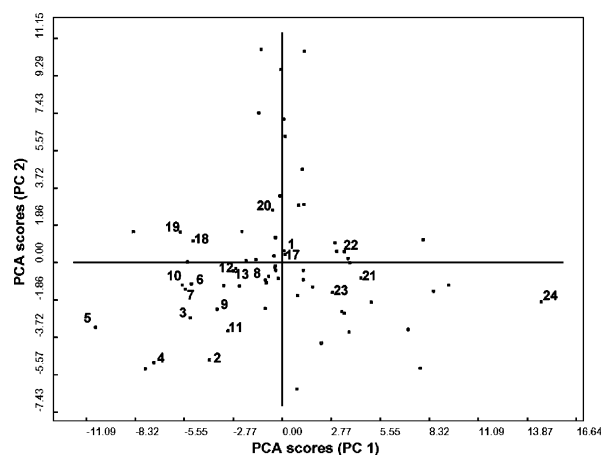


Figure 1. PCA score plot for 67 coumarin derivatives.

ated a series of coumarins. Values of IC<sub>50</sub> were independently determined by making rate measurements for at least five inhibitor concentrations. The values were estimated from the collected data using the nonlinear curve-fitting program SigmaPlot 2001 7.0. The method of partial least square (PLS) regression was used to analyze the 24 compounds shown in Table 1 by correlating variations in their biological activity with variations in their interaction fields. The model was evaluated

Table 1.

Compound	Structure <sup>a</sup>	Actual <sup>b</sup> (log 1/IC <sub>50</sub> )	VolSurf calculated	VolSurf residuals
1 (Chalepin)		4.26	4.12	−0.14
2		3.59	3.72	0.13
3		3.46	3.69	0.23
4		3.21	3.53	0.32
5		3.16	3.34	0.18
6		3.84	3.72	−0.12
7		3.71	3.71	0.00
8		4.13	4.03	−0.10
9		3.91	3.79	−0.12

Table 1. (continued)

Compound	Structure <sup>a</sup>	Actual <sup>b</sup> (log 1/IC <sub>50</sub> )	VolSurf calculated	VolSurf residuals
10		3.89	3.75	−0.14
11		3.79	3.83	0.04
12		3.72	3.89	0.17
13		3.68	3.89	0.21
14		4.19	4.26	0.07
15	14, R =	4.25	4.56	0.31
16	14, R =	4.25	4.32	0.07
17		4.51	4.15	−0.35
18	17, R <sub>1</sub> = R <sub>2</sub> = R <sub>3</sub> = R <sub>4</sub> = R <sub>6</sub> = H, R <sub>5</sub> = OH	4.17	3.86	−0.31
19	17, R <sub>1</sub> = R <sub>2</sub> = R <sub>3</sub> = R <sub>5</sub> = R <sub>6</sub> = H, R <sub>4</sub> = OH	4.41	3.81	−0.61
20	17, R <sub>1</sub> = OAc, R <sub>2</sub> = R <sub>3</sub> = R <sub>4</sub> = R <sub>5</sub> = R <sub>6</sub> = H	3.91	4.09	0.18
21	17, R <sub>1</sub> = R <sub>5</sub> = OAc, R <sub>2</sub> = R <sub>3</sub> = R <sub>4</sub> = R <sub>6</sub> = H	4.77	4.41	−0.36
22	17, R <sub>1</sub> = R <sub>4</sub> = OAc, R <sub>2</sub> = R <sub>3</sub> = R <sub>5</sub> = R <sub>6</sub> = H	4.28	4.31	0.04
23	17, R <sub>1</sub> = OAc, R <sub>5</sub> = OMe, R <sub>2</sub> = R <sub>3</sub> = R <sub>4</sub> = R <sub>6</sub> = H	4.07	4.27	0.20
24	17, R <sub>1</sub> = R <sub>2</sub> = R <sub>4</sub> = R <sub>5</sub> = OAc, R <sub>3</sub> = R <sub>6</sub> = H	4.75	4.86	0.11

<sup>a</sup> Compounds 1–13 have been previously described.<sup>12</sup> The detailed synthesis of compounds 14–24 will be published elsewhere.

<sup>b</sup> IC<sub>50</sub> values were determined according to the previously described procedures.<sup>12,13</sup> The inhibitor concentration required for 50% inhibition (IC<sub>50</sub>) was calculated from at least five inhibitor concentrations.

by the non-cross-validated correlation coefficient,  $r^2 = 0.689$ ; cross-validated correlation,  $q^2 = 0.603$  (via LOO procedure, which drops to 0.592 when five random groups are left out); standard deviation of error of calculation, SDEC = 0.230; and standard deviation of error of predictions, SDEP = 0.260, respectively. These statistical results suggest a good correlation between the VolSurf descriptors (hydrophobic and hydrophilic fields) and the biological activities of the compounds studied. Figure 2 shows the PLS plot of  $T$  versus  $U$  for

the first component. It is interesting to note that the two most potent compounds, **21** and **24**, are located in the upper-right portion of  $T$ – $U$  positive values, whereas the less potent ones, **4** and **5**, are in the opposite direction.

The model was further evaluated through the inclusion of a series of 26 nucleosides and 27 flavonoids. H<sub>2</sub>O and hydrophobic DRY probes were applied in the VolSurf method as earlier described.<sup>10</sup> The investigation of the interactions of molecules with a virtual receptor site

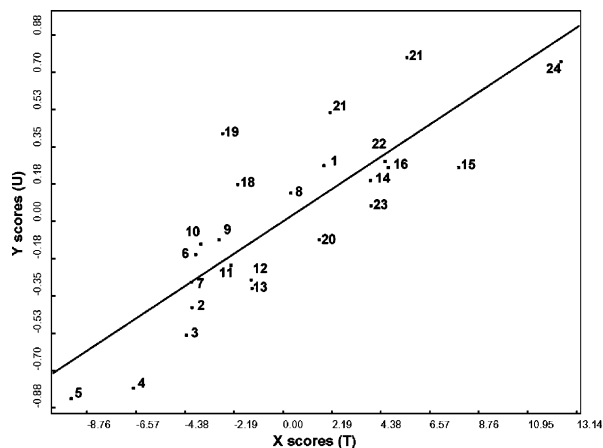


Figure 2. PLS plot of *T* versus *U* for one component.

(VRS) has been a useful visual interface for enhancing the ability to design and prioritize new lead candidates, considering the relationships between molecular interaction fields (MIF) and biological activity. This was accomplished by calculating the VRS for the new dataset that was subsequently predicted by the previous VRS. This is simply done by validating the late VRS with the first one. Results show that this is the case for the set of molecules employed in this study. Figure 3 shows the external PCA prediction scores for the first two components for 13 training chalepin (1) analogues along with the nucleoside and flavonoid molecules. Again, PC1 accounts for 30% of total variance.

The PCA score plot from Figure 3 shows each 3D structure represented by a single point clustered according with PC1, which is capable of classifying the chalepin analogues in the range from  $-10.32$  to  $-1.54$

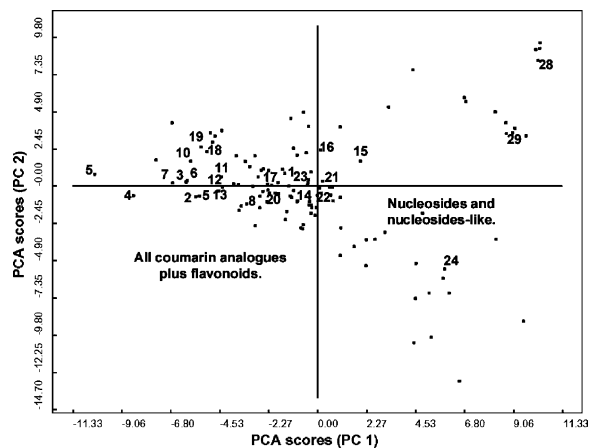


Figure 3. External PCA prediction score plot for 13 training coumarins.

PC1 scores, whereas the nucleosides are in the upper positive values of PC1. The majority of the flavonoids are clustered right in the middle of the graph, just between coumarins and nucleosides. It is worth to note that coumarin **24** is clustered along with the nucleosides. The results depicted in the Figure 3 show that the potency increases as the PC1 values become more positive, thus allowing the straightforward identification of possible structural modifications to improve potency and selectivity against *T. cruzi* GAPDH.

To further test the predictive ability of the model, three new compounds reported by Kennedy et al.<sup>14</sup> were included in our data set (**25**, **26**, **27**). These compounds, along with the two most potent nucleoside-like compounds (**28**, **29**) synthesized by us were clustered at the very same positive values of PC1 (graph not shown).

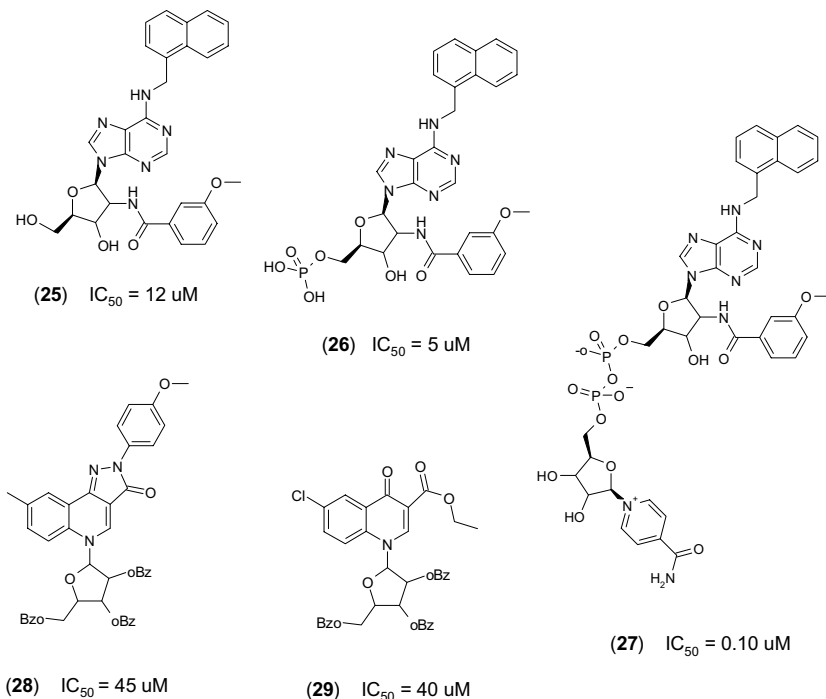


Figure 4.  $IC_{50}$  values for the compounds used to further test the predictive quality of the model.

Figure 4 shows the structures of this small set. The IC<sub>50</sub> values were measured under similar conditions as previously described.<sup>12,13</sup>

Additionally, a series of 17 inhibitors of GAPDH (adenosine analogues) described by Bressi et al.<sup>15</sup> possessing the ability to block the growth of cultured *T. brucei* and *T. cruzi*, were also used to evaluate our model (graph not shown). The results were substantially in agreement with those of previous PCA/PLS analyses with respect to the first component, as thoroughly depicted in this paper.

So far, we have presented the use of the VolSurf method for the investigation of the interactions of molecules according with a VRS. In the following example, we evaluate the binding site of the enzyme by the generation of a pharmacophoric model using the same probes. This work was possible due to the availability of high-resolution crystal structures of GAPDH. The MIF were generated only for the receptor site using the amino acid side chains flexibility mode in GRID (directive MOVE = 1).<sup>16</sup>

High selectivity is an essential requirement in chemotherapy, and should be considered as early as possible in drug design. The structural features of the ligands that play a key role for selectivity are therefore of great importance. The parasite and human GAPDHs are structurally different, thus opening the possibility for the design of potent and selective inhibitors.<sup>8,9</sup>

The VolSurf descriptors were applied once again in the study involving four 3D structures of GAPDH, including human, *T. cruzi*, *T. brucei*, and *L. mexicana* (PDB codes 3GPD, 1K3T, 1GGA, and 1I32, respectively). Based on the 3D structures of the proteins, this method analyzes selectivity differences from the view of the receptor and is therefore independent of the availability of appropriate ligands for a ligand-based QSAR analysis. The use of PCA<sup>17</sup> allows visual interpretation of the results to guide the understanding of the contributions of various interactions in the binding process (Fig. 5).

Pharmacokinetic properties were also evaluated according to procedures previously described.<sup>18–20</sup> We carried out a MIF projection for the 24 coumarins depicted in Table 1 using the built-in pharmacokinetic models (Caco-2 and human intestinal absorption, HIA) implemented in the VolSurf program. The result of the %HIA PLS score plot is shown in Figure 6A. The data demonstrate that the 24 coumarins can be regarded as having high probability of being absorbed in such a system. Similar results were also found for the Caco-2 model, as shown in Figure 6B.

Overall, very similar PCA loading profile plots are found for PC1 of all compounds. Since the reported strategy is able to rapidly predict biological potency, the VolSurf method can be applied to large ligand series. The pertinent differences responsible for selectivity can be directly translated into suggestions on how an existing ligand can be modified to enhance selectivity toward

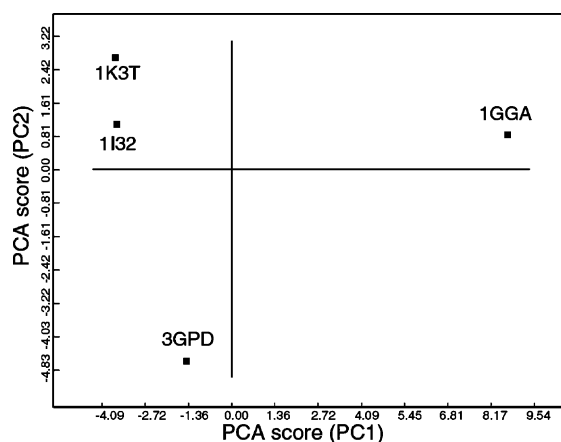
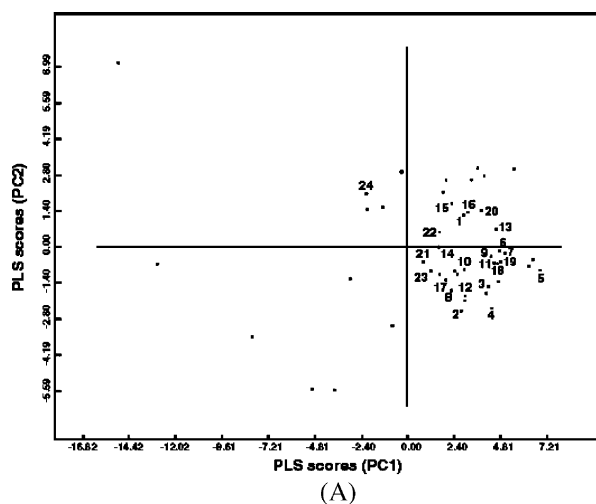
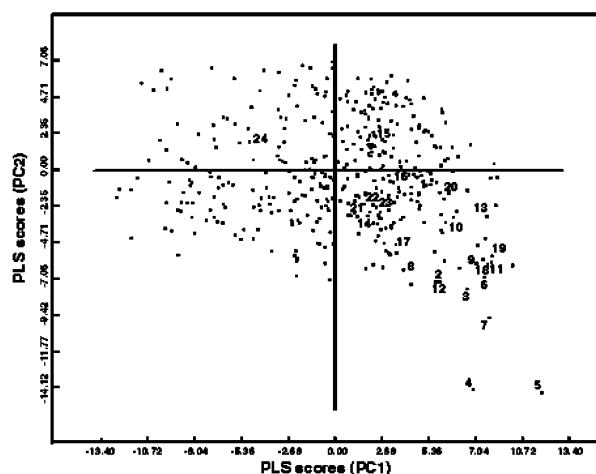


Figure 5. PCA score plot for H<sub>2</sub>O and hydrophobic DRY probes.



(A)



(B)

Figure 6. PLS score plot models for the projection of 24 coumarins. (A) %HIA; and (B) Caco-2 cells.

a given target. Combined receptor- and ligand-based 3D QSAR is an interesting approach for future drug design studies. The VolSurf method appears as a valuable filter

in evaluating pharmacokinetic profile of promising compounds.

### Acknowledgements

We thank the CNPq (Conselho Nacional de Desenvolvimento Científico e Tecnológico), FAPESP (Fundação de Amparo à Pesquisa do Estado de São Paulo), and FAPEMIG (Fundação de Amparo à Pesquisa do Estado de Minas Gerais), for financial support.

### References and notes

1. Coura, J. R.; Castro, S. L. *Mem. Inst. Oswaldo Cruz* **2002**, *97*, 3–24.
2. Verlinde, C. L. M. J.; Bressic, J. C.; Choe, J.; Suresh, S.; Buckner, F. S.; Van Voorhis, W. C.; Michels, P. A. M.; Gelb, M. H.; Hol, W. G. J. *J. Braz. Chem. Soc.* **2002**, *13*, 843–848.
3. Yun, M.; Park, C.-G.; Kim, J.-Y.; Park, H.-W. *Biochemistry* **2000**, *39*, 10702–10710.
4. Mercer, W. D.; Winn, S. I.; Watson, H. C. *J. Mol. Biol.* **1976**, *104*, 277–283.
5. Vellieux, F. M.; Hajdu, J.; Verlinde, C. L. M. J.; Groendijk, H.; Read, R. J.; Greenhough, T. J.; Campbell, J. W.; Kalk, K. H.; Littlechild, J. A.; Watson, H. C.; Hol, W. G. J. *Proc. Natl. Acad. Sci. USA* **1993**, *90*, 2355–2359.
6. (a) Pavão, F.; Castilho, M. S.; Pupo, M. T.; Dias, R. L. A.; Correa, A. G.; Fernandes, J. B.; da Silva, M. F. G. F.; Mafezoli, J.; Vieira, P. C.; Oliva, O. *FEBS Lett.* **2002**, *520*, 13–17; (b) Souza, D. H. F.; Garratt, R. C.; Araújo, A. P. U.; Guimarães, B. G.; Jesus, W. D. P.; Michels, P. A. M.; Hannaert, V.; Oliva, G. *FEBS Lett.* **1998**, *424*, 131–135.
7. Kim, H.; Feil, I. K.; Verlinde, C. L. M. J.; Petra, P. H.; Hol, W. G. J. *Biochemistry* **1995**, *34*, 14975–14986.
8. Suresh, S.; Bressi, J. C.; Kennedy, K. J.; Verlinde, C. L. M. J.; Gelb, M. H.; Hol, W. G. J. *J. Mol. Biol.* **2001**, *309*, 423–435.
9. Verlinde, C. L.; Merritt, E. A.; Van den Akker, F.; Kim, H.; Feil, I.; Delboni, L. F.; Mande, S. C.; Sarfaty, S.; Petra, P. H.; Hol, W. G. *Protein Sci.* **1994**, *3*, 1670–1686.
10. Menezes, I. R. A.; Lopes, J. C. D.; Montanari, C. A.; Oliva, G.; Pavão, F.; Castilho, M. S.; Vieira, P. C.; Pupo, M. T. *J. Comput. Aided Mol. Des.* **2003**, *17*, 277–290.
11. Zamora, I.; Oprea, T.; Cruciani, G.; Pastor, M.; Ungell, A.-L. *J. Med. Chem.* **2003**, *46*, 25–33.
12. Vieira, P. C.; Mafezoli, J.; Pupo, M. T.; Fernandes, J. B.; da Silva, M. F. G. F.; Albuquerque, S.; Oliva, G.; Pavão, F. *Pure Appl. Chem.* **2001**, *3*, 617–622.
13. Aronov, A. M.; Verlinde, C. L. M. J.; Hol, W. G. J.; Gelb, M. H. *J. Med. Chem.* **1998**, *41*, 4790–4799.
14. Kennedy, K. J.; Bressi, J. C.; Gelb, M. H. *Bioorg. Med. Chem. Lett.* **2001**, *11*, 95–98.
15. Bressi, J. C.; Verlinde, C. L. M. J.; Aronov, A. M.; Shaw, M. L.; Shin, S. S.; Nguyen, L. N.; Suresh, S.; Buckner, F. S.; Van Voorhis, W. C.; Kuntz, I. W.; Hol, W. G. J.; Gelb, M. H. *J. Med. Chem.* **2001**, *44*, 2080–2093.
16. GRID V.20, Molecular Discovery Ltd, 2002 (<http://www.moldiscovery.com>).
17. Wold, S.; Esbensen, K.; Geladi, P. *Chemom. Intell. Lab. Syst.* **1987**, *2*, 37–52.
18. Ooms, F.; Weber, P.; Carrupt, P.-A.; Testa, B. *Biochim. Biophys. Acta* **2002**, *1587*, 118–125.
19. Cruciani, G.; Crivori, P.; Carrupt, P.-A.; Testa, B. *J. Mol. Struct. Theochem.* **2000**, *503*, 17–30, Sp. Iss.
20. Cruciani, G.; Pastor, M.; Guba, W. *Eur. J. Pharma. Sci.* **2000**, *11*(Suppl. 2), S29–S39.